



Olive mill wastewater concentration by two-stage reverse osmosis in tubular configuration, in a scheme combining open and tight membranes

Konstantinos B. Petrotos*, Maria I. Kokkora, Chryssoula Papaioannou,
Paschalis E. Gkoutosidis

Laboratory of Food and Biosystems Engineering, Department of Agricultural Engineering Technologies, Technological Educational Institute of Thessaly, TEI Campus, 41100 Larissa, Greece, Tel. +30 2410 684524; Fax: +30 2410 613158; email: petrotos@teilar.gr (K.B. Petrotos)

Received 25 September 2015; Accepted 7 November 2015

ABSTRACT

A novel concept for olive mill wastewater (OMWW) concentration, involving the combination of open and tight reverse osmosis (RO) membranes in tubular configuration, was studied. The OMWW, prior to RO concentration, was clarified in two successive steps: passing through a coarse rotating finisher and by ceramic microfiltration, in order to remove suspended matter and facilitate the RO concentration. The clarified raw material was then concentrated using the tubular PCI UK AFC40 RO membrane. A parametric study was conducted to investigate the effect of main process parameters on permeation flux. The permeation flux of AFC40 RO membrane was found to reach consistently high values without substantial membrane fouling problems. Furthermore, the parametric study proved that the flux was linearly increased by increasing the transmembrane pressure, and exponentially decreased by increasing the OMWW mass concentration factor. In most cases, the permeation flux increased with increasing flow velocity. The effect of temperature on permeation flux was depended on both transmembrane pressure and flow velocity. The AFC40 permeate content of total dissolved solids (TDS) was approximately 0.6%, which accounts for roughly 15% of the TDS in the initial OMWW solution. The AFC40 permeate was, therefore, further concentrated using the AFC99 PCI UK tight RO membrane, aiming to obtain a permeate suitable for disposal to natural resources, whilst simultaneously reclaiming valuable antioxidants by mixing the two retentates of AFC40 and AFC99 membranes. The results of this study show that the proposed two-stage RO scheme may be potentially applied in a commercial scale and contribute towards processing of OMWW to produce liquid antioxidant and water suitable for disposal to natural resources.

Keywords: Olive mill waste water (OMWW); Membrane concentration; Tubular reverse osmosis; Mathematical modelling

1. Introduction

Olive oil production is one of the main agricultural activities in the Mediterranean basin countries. There

are approximately 750 million productive olive trees (*Olea europaea* L.) worldwide, with the countries of the Mediterranean basin concentrating 97% of the world olive oil production [1]. In parallel, it has been estimated that more than $30 \times 10^6 \text{ m}^3$ of oil mill waste is produced annually in the Mediterranean region, with

*Corresponding author.

Spain, Italy and Greece being the largest producers [2]. This dark-coloured olive mill liquid effluent (OMWW) poses a significant environmental hazard, as the seasonality of olive oil production and the characteristics of wastewater (very high chemical oxygen demand, $\text{COD} > 80 \text{ g L}^{-1}$, total suspended solids, $\text{TSS} > 20 \text{ g L}^{-1}$, acidic pH 4–5, phenolic compounds $1.5\text{--}10 \text{ g L}^{-1}$) make its management difficult and costly [3,4]. However, this potentially harmful effluent, for the ecosystem, can serve, if properly managed, as an inexpensive and convenient source of natural antioxidants, mainly due to its high polyphenolic content. Polyphenols are water-soluble organic compounds and, therefore, they are found in higher concentration in OMWW than in olive oil itself [5,6]. So far, more than 40 phenols have been identified in OMWW, such as hydroxytyrosol, tyrosol, caffeic acid and p-coumaric acid. Hydroxytyrosol is considered the main natural polyphenolic compounds due to its high bio-antioxidant capacity [7]. Moreover, as natural substances, their high-potential antioxidant properties are reflected in their high market price, and their great demand in the cosmetic, pharmaceutical and food industry.

Up to now, various treatment processes for the management and reclamation of OMWW have been proposed [8]. Biological treatment of OMWW is a hard task and right now not applied on a large scale, due to the resistance of OMWW to biological degradation [9–13]. Other treatment practices have been developed, such as lagooning or natural evaporation and thermal concentration [14,15], treatments with lime and clay [16,17], composting [18–20], physicochemical procedures as coagulation–flocculation [21–23] and electrocoagulation [24,25], advanced oxidation processes, including ozonation [26], Fenton's reagent [27,28] and photocatalysis [29] and also electrochemical [30–32] and hybrid processes [33–36]. Most of the above-mentioned technologies face the OMWW as a waste that must be destroyed and not to be used as a raw material for the production of high added value products and simultaneously reclaim valuable water resources. In contrast to this approach, membrane technologies, which are developed within the last decade, attempt to utilize the OMWW for production of valuable antioxidant and clean water, according to the EU principle of total discharge of the waste materials.

As it is cited by Zagklis et al. [37], membranes have been implemented for the purification of olive mill wastewater (OMWW) by many researchers and mostly not as a plain technology, but as a combination, with some of them trying to isolate and purify the phenolic compounds contained. Russo [38] tested a membrane

system consisting of microfiltration (MF), ultrafiltration (UF) and reverse osmosis (RO), where the low-molecular weight phenols were concentrated in the RO step and also proposed the addition of a nanofiltration (NF) step before RO, where phenols could be concentrated instead. The final product had a concentration of free low-molecular weight phenols at 0.5 g L^{-1} , with 80% being hydroxytyrosol. Garcia-Castello et al. [39] proposed a system consisting of MF, NF and osmotic distillation (OD)/vacuum membrane distillation. The low-molecular weight phenols were concentrated to 0.5 g L^{-1} in the OD step, with 56% being hydroxytyrosol. Conidi et al. [40] combined an MF and UF system followed by a multiphase biocatalytic membrane reactor (MBMR) system for the conversion and separation of oleuropein to oleuropein-aglycon. The conversion achieved in the MBMR step was 45.7% for a feed concentration of 545 mg L^{-1} oleuropein. El-Abbassi et al. [41] proposed the use of membrane distillation for the concentration of all compounds contained in the waste, including phenols, and the removal of clear water. Cassano et al. [42] tested the effect of UF membranes used for the separation of phenols from OMWW and proposed an integrated membrane system, consisting of two sequential UF steps and finally an NF membrane for the concentration of OMWW phenols with a final concentration of 960 mg L^{-1} [42,43]. In previous works [44,45], the combination of UF–NF/RO was examined resulting to a final phenol concentration of 10 g L^{-1} . Moreover, combined membrane schemes including either MF in combination with UF and NF [46] or UF and NF [47] were used targeting high added value hydroxytyrosol production.

The aim of the present work was to comprehensively investigate a novel scheme of concentration of initially MF clarified OMWW, using a two-step tubular RO technology, employing a low rejection membrane in the first stage and a high rejection tight RO membrane as a second step for polishing the permeate of the first step and reclaiming pure water and concentrated antioxidant solution with very low fouling effects.

2. Materials and methods

2.1. Olive mill wastewater

Samples of OMWW were taken from a local olive mill at Pournari village, Larissa, central Greece, in December 2014. The samples were taken directly from the output stream of the three-phase decanter centrifugal of the olive mill, and they were stored in twenty 25-L plastic bottles at a temperature of 2°C .

2.2. OMWW pre-treatment

Due to high TSS and sludge content of OMWW, the OMWW samples were initially centrifuged, using a rotating finisher equipped with a stainless steel screen with openings of 150 μm diameter, in order to remove the sludge naturally contained in the OMWW.

In the second step of the pre-treatment process, the liquid, which had passed through the finisher and still contained oil residuals, was micro-filtered in a tangential flow ceramic MF module, type CMV 3–30 equipped with three ceramic membranes type CMF19040—200 nm with a total filtration area of 0.69 m^2 , in order to remove oil residuals and the remaining large size suspended solids. The Chinese company Jiangsu Jiuwu Hi-Tech Co. Ltd supplied this module, along with the membranes. The MF process continued until approximately 80% of the initial volume was collected as permeate. The operating conditions of MF were: transmembrane pressure 3.5 bar, temperature 40°C and flow velocity 10 m s^{-1} . The obtained micro-filtrate was then used as a raw material for the RO experiments. OMWW micro-filtrate contained 96.2% water, 0.55% polyphenols, 3.05% total carbohydrates, 0.2% proteins and no fat (0%), since the use of the 0.2- μm pore size diameter concentrated the oil to the retentate.

2.3. Tubular RO membranes

Two respective tubular RO membranes were used: (a) The low rejection AFC40 RO membrane (open RO membrane), which was a thin-film composite type of membrane having aromatic polyamide top selective layer, pH resistivity from 1.5 to 9.5, allowed maximum operation temperature 60°C and maximum operation pressure 60 bar and apparent retention 60% as CaCl_2 . The retention capability of the AFC40 RO membrane was relatively low, within the range of nano-filtration, and (b) The AFC99 tight RO membrane, which was a thin-film composite type of membrane having aromatic polyamide top selective layer, pH resistivity from 1.5 to 12.0, allowed maximum operation temperature 80°C and maximum operation pressure 64 bar and apparent retention 99% as NaCl .

Both membranes were of 1.2 m length and of 0.0125 m diameter (effective membrane surface of 0.88 m^2). Also, both membranes were used in sets of 18 pieces each.

2.4. Description of RO experimental rig and experimental sequence

The RO experimental rig is presented in Fig. 1. It consisted of the following components:

- (1) A high-pressure positive displacement plunger pump, with three plungers and model power sprayer manual type TF-100, which was capable of producing a pressure from 0 to 40 bar and delivering the liquid at 150 L min^{-1} . The pump was equipped with a pressure relief valve.
- (2) An electronic inverter connected to the pump type ELECTRO ADDA SPA, Italy.
- (3) Two tubular membrane modules, type B1 by PCI UK. One of the two modules was operating in series flow and accommodated 18 AFC40 low rejection RO membrane tubes, and the second with twin-entry type flow and accommodated 18 AFC99 tight, high rejection RO membrane tubes. The first module was used for the experimentation with the low rejection AFC40 RO membrane and the second for the experiments with the AFC99 high rejection RO membrane.
- (4) A 500-L capacity stock tank, where the OMWW micro-filtrate was accommodated. The tank was equipped with heating and cooling facilities and automatic temperature control in order to control the temperature of the processed OMWW.
- (5) A back pressure valve, located at the output of the two modules, used to adjust the operating pressure at the required value.
- (6) A set of food grade, high-pressure (externally reinforced with metallic cover), plastic tubes, used to connect the above-mentioned components and form the experimental rig. All the tube connections were of safe type and leakage proof for high-pressure operation.

The experimental methodology involved initially the investigation of membrane fouling problems. The two membranes were left to operate for at least 1 h at a medium pressure of 20 bar, tangential velocity during cross-flow filtration (flow velocity) of 5.5 m s^{-1} and temperature of 35°C, in order to stabilize and surpass the first stage of high flux vs. time reduction, which represents the build-up of the fouling layer on the membrane. At these conditions, the flux measurement was repeated several times within the experimental course, in order to collect data for the membrane fouling.

As a second step, the permeation flux was measured under different conditions of temperature, flow velocity and transmembrane pressure. Specifically, three temperature settings: 25, 35 and 45°C were combined with four flow velocities: 4.1, 5.5, 6.9 and

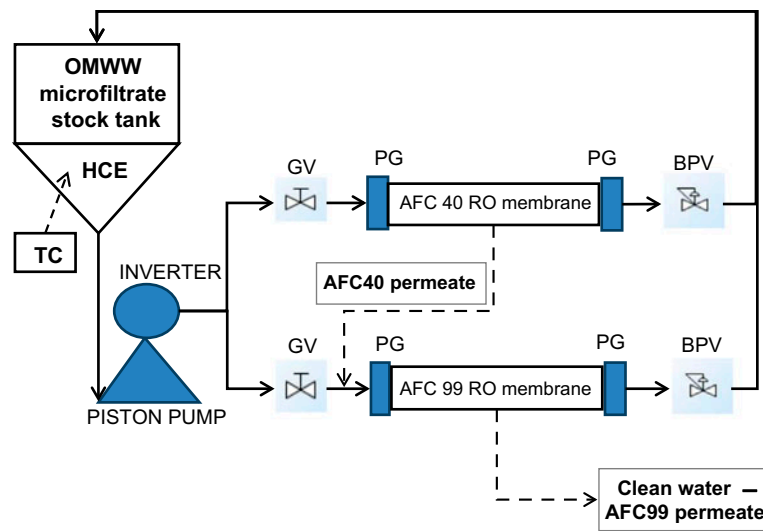


Fig. 1. The RO experimental rig (TC: temperature control, GV: gate valve, BPV: back pressure valve, PG: pressure gauge, HCE: heating/cooling element).

8.3 m s^{-1} and four transmembrane pressure settings: 10, 20, 30 and 40 bar.

Furthermore, the mass concentration ratio (MCR), at time t (in minutes) from the beginning of the concentration, was determined as the ratio of the initial mass of OMWW micro-filtrate (kg of OMWW micro-filtrate originally placed in the stock tank at $t = 0$) to the mass of OMWW micro-filtrate at time t minutes from the beginning of the experiment, which was calculated by subtracting the mass (kg) of RO permeate (first RO module) at time t from the mass of OMWW micro-filtrate at $t = 0$. In order to evaluate the effect of MCR on the RO permeation flux, the transmembrane pressure was adjusted to 30 bar, the operation temperature to 35°C and two respective sets of data were taken at flow velocities of 4.1 and 6.9 m s^{-1} , at four MCRs: 1 (non-concentrated OMWW), 1.17, 1.41 and 1.77.

Moreover, a comparison of the performance of two RO membranes—AFC40 and AFC99—was carried out. The permeation flux of the two membranes was determined under the following operating conditions: flow velocity 4.1 m s^{-1} , temperature 35°C and transmembrane pressure of 10 bar, 20 bar and 25 bar.

Finally, the RO permeate of the AFC40 was concentrated using the tight AFC99 RO membrane at transmembrane pressure 40 bar, temperature 45°C and flow velocity 6.9 m s^{-1} , in order to evaluate if the average permeation flux is of commercial magnitude.

Measurements of the total antioxidant activity of the initial OMWW micro-filtrate, AFC40 permeate and AFC99 retentate were measured using the standard method [48], in order to determine the recovery of the

high added value antioxidants using the combined open and tight RO membrane operation schemes.

The membrane permeation flux value was calculated at all times using Eq. (1):

$$\text{Flux (kg m}^{-2} \text{ h}^{-1}) = 12 \times \frac{M_5}{A} \quad (1)$$

where A is the membrane area in m^2 , and M_5 is the mass of permeate collected within 5 min.

2.5. Membrane cleaning regime

The membrane cleaning regime for both membranes consisted of the following steps:

- (1) Rinsing with de-ionized water for 15 min.
- (2) Filling of the stock tank with hot water at 48°C .
- (3) Addition of Ultrasil 69 (0.36%), Ultrasil 67 (0.16%), Ultrasil 02 (0.04%), one after another, with simultaneous stirring and circulation for 45 min.
- (4) Rinsing with hot water at 48°C .
- (5) Filling of the stock tank with hot water at 48°C .
- (6) Addition of acidic cleaner Ultrasil 75 (0.12%) with simultaneous stirring and circulation for 15 min.
- (7) Rinsing with hot water at 48°C .
- (8) Filling of the stock tank with hot water at 48°C .
- (9) Addition of alkali cleaner Ultrasil 110 (0.24%) with simultaneous stirring and circulation for 15 min.

- (10) Rinsing with hot water at 48°C.
- (11) Membrane preservation with 0.1% sodium bisulphate solution to prevent microbial growth.

All the cleaner solutions used were purchased from HENKELECOLAB, Greece. This cleaning regime was proved effective in restoring the membrane performance after its long-term operation (operation time over 12 h).

3. Results and discussion

3.1. Comparative flux values and rejection factors for concentration with AFC40 and AFC99 tubular RO membranes

The comparison of the performance of two RO membranes AFC40 and AFC99 is graphically represented as the flux vs. transmembrane pressure in Fig. 2. The AFC40 RO membrane resulted in substantially higher performance than the AFC99, with the flux value being more than fourfold higher under the same operating conditions for AFC40 RO membrane. For this reason, it was chosen to conduct the OMWW micro-filtrate concentration study using the AFC40 membrane and use the AFC99 for the concentration of the low-concentration permeate of the AFC40.

Furthermore, the retentions of total dissolved solids (TDS) by the two respective RO membranes were also different. The permeate of the AFC40 contained about 0.6% w/w TDS, which counted for 18% of the concentration of the OMWW micro-filtrate

(3.3% w/w) or 82% retention. On the other hand, the retention achieved using the AFC99 RO membrane was almost 100%.

3.2. The effect of transmembrane pressure on permeation flux of AFC40 membrane

The effect of the transmembrane pressure on the RO permeation flux of AFC40 membrane is presented in Fig. 3, taking into consideration the effect of flow velocity. The permeation flux increased linearly with increasing transmembrane pressure. The maximum flux value was $165 \text{ kg m}^{-2} \text{ h}^{-1}$ and it was achieved at transmembrane pressure of 40 bar (temperature 25°C and flow velocity 8.3 m s^{-1}). This flux value is considered to be high and suitable for commercial application of the RO for the concentration of clarified OMWW.

3.3. The effect of flow velocity on permeation flux of AFC40 membrane

In general, the AFC40 permeation flux was found to increase with increasing flow velocity. It was observed that at lower temperature, this increase of flux between the lower and higher flow velocity was more substantial (Fig. 4). At the temperature of 45°C and transmembrane pressure of 40 bar, however, the higher flow velocity resulted in decreased permeation flux, potentially due to concentration polarization. The graphical representation of the ratio flux/flow velocity vs. flow velocity showed the exponential relationship of the two parameters (Fig. 5).

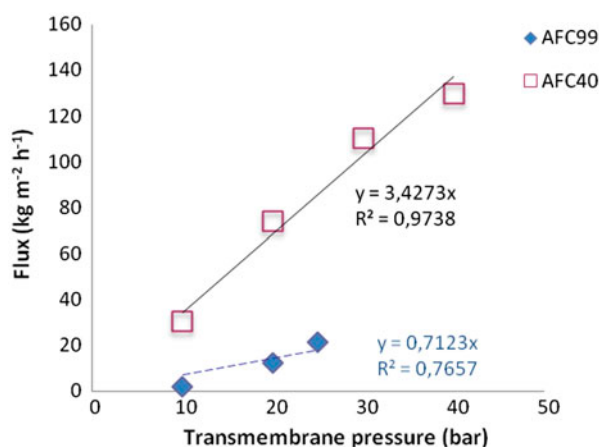


Fig. 2. The effect of transmembrane pressure on permeate flux for the AFC40 and AFC99 RO membranes. The OMWW flow velocity was 4.1 m s^{-1} and the temperature was 35°C.

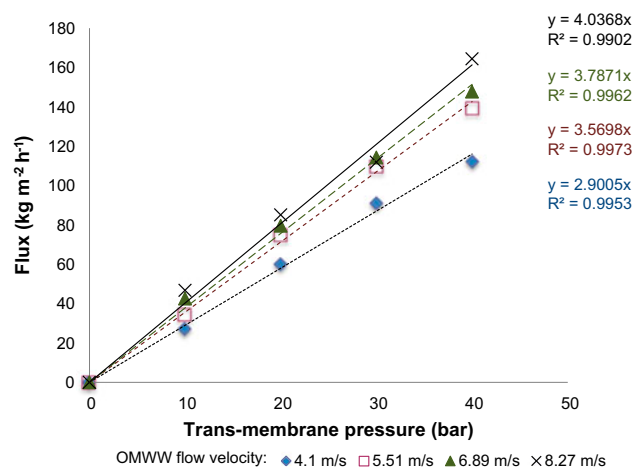


Fig. 3. The variation of permeate flux of the AFC40 RO membrane on different transmembrane pressure values as affected by OMWW flow velocity at temperature of 25°C.

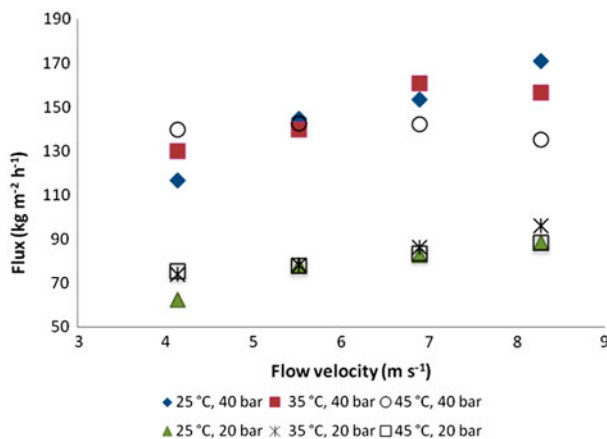


Fig. 4. The effect of OMWW micro-filtrate flow velocity on permeate flux of the AFC40 RO membrane, for different conditions of temperature (25, 35 and 45°C) and transmembrane pressure (20 and 40 bar).

3.4. The effect of operating temperature on permeation flux of AFC40 membrane

OMWW micro-filtrate permeation flux of the AFC40 RO membrane was found depended on operating temperature, but it did not follow an Arrhenius relationship, as it is commonly observed for RO membranes. It is apparent from the data presented in Fig. 6 that the effect of temperature on permeation flux was depended on both transmembrane pressure and flow velocity. In general, the increase in temperature resulted in increased flux in the case of flow velocity of 4.1 m s⁻¹, irrespectively of transmembrane pressure. The increased flux with increasing flow velocity at constant transmembrane pressure was attributed to lower polarization effect. The flux was practically not influenced by temperature at flow velocity of

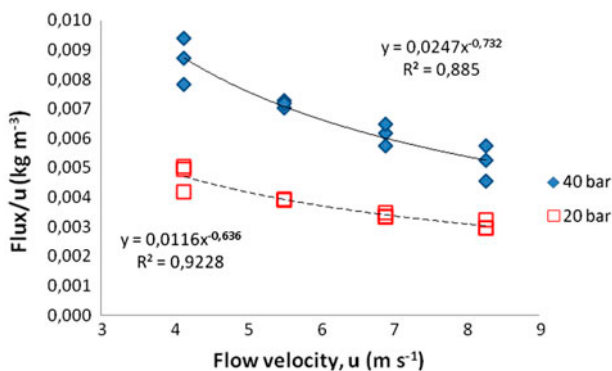


Fig. 5. The exponential relationship between OMWW micro-filtrate flow velocity (u) and the quotient of permeate flux/ u .

5.5 m s⁻¹, irrespectively of transmembrane pressure. In the case of flow velocity of 6.9 and 8.3 m s⁻¹ and transmembrane pressure 30 and 40 bar, the increase in temperature over 35°C resulted in decreased flux. Furthermore, in the case of pressure 40 bar and flow velocity 8.3 m s⁻¹, the permeation flux reduced from a value over 170 kg m⁻² h⁻¹ at 25°C to less than 140 kg m⁻² h⁻¹ at 45°C. The reduction of the permeation flux with increase in temperature, at higher pressures and flow velocities, was probably due to membrane compaction.

3.5. The effect of mass concentration on permeation flux of AFC40 membrane

The effect of MCR on permeate flux was determined for two respective settings under experimental conditions: (a) at 35°C, 30 bar and 4.1 m s⁻¹, and (b) at 35°C, 30 bar and 6.9 m s⁻¹. As shown in Fig. 7, a rapid reduction in the permeation flux with increasing MCR was observed. Permeation flux decreases exponentially with increasing MCR, in both conditions studied.

3.6. The fouling of AFC40 and AFC99 membranes

In order to assess potential fouling problems of the AFC40 membrane, a set of measurements of the permeation flux were taken at transmembrane pressure of 20 bar, temperature of 35°C and flow velocity of 5.6 m s⁻¹, in a course of 5 h and 15 min (Fig. 8). The permeation flux was measured several times within this time period. The results indicated that the fouling effect was not substantial when the AFC40 membrane was used for the concentration of OMWW micro-filtrate, probably due to the effect of the clarification and oil residues removal by the ceramic MF membrane.

The same effect was also observed in the case of concentration of the AFC40 permeate using the AFC99 RO membrane. In this case, the permeation flux observed was higher than 60 kg m⁻² h⁻¹ (data not shown). This value appears to be four times higher than the permeation flux measured in the case of concentrating OMWW micro-filtrate with the AFC99 RO membrane.

3.7. Mathematical modelling of RO concentration by AFC40 tubular membrane

A mathematical model was developed to predict the permeation flux values for the RO concentration of OMWW micro-filtrate by the AFC40 tubular RO membrane. The general form of the modelling equation was based in the above-mentioned experimentally

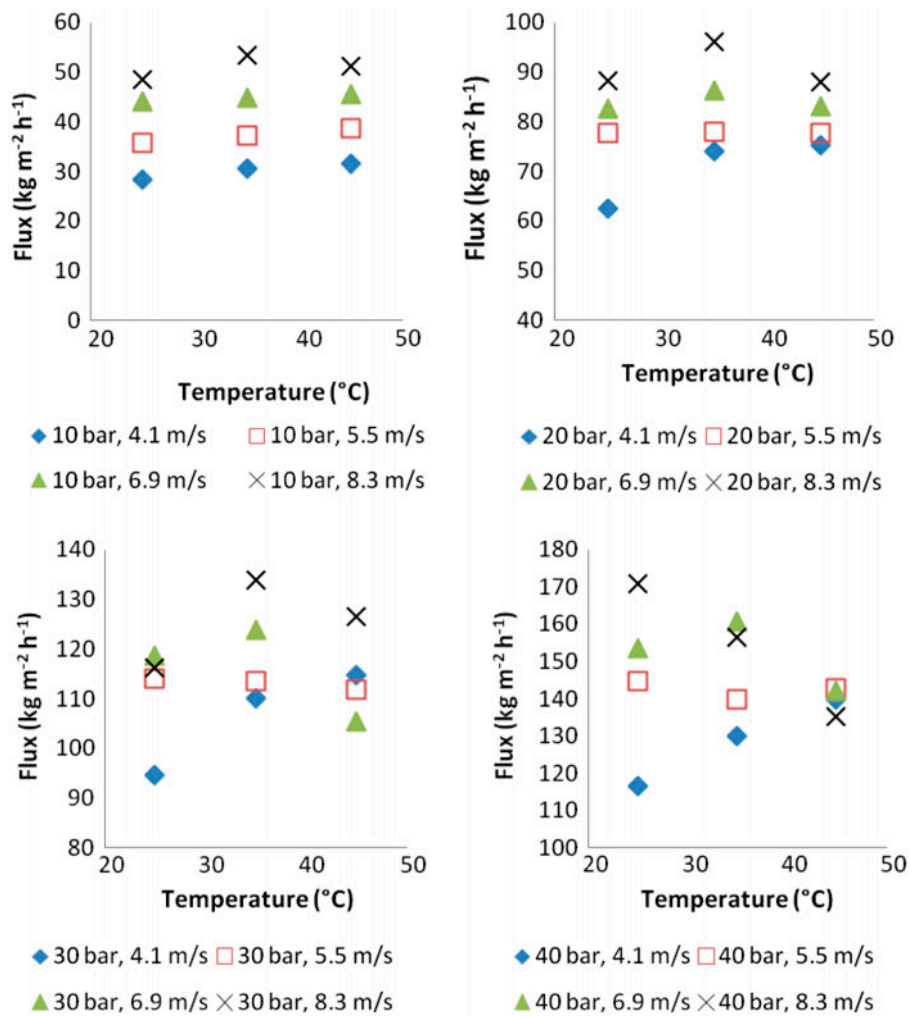


Fig. 6. AFC40 RO membrane permeate flux fluctuation with temperature, for different conditions of OMWW micro-filtrate flow velocity and transmembrane pressure.

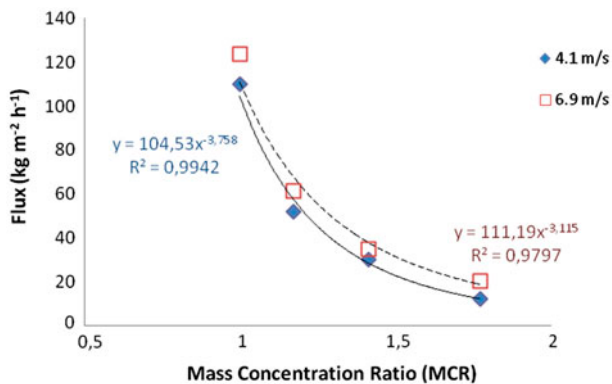


Fig. 7. The effect of OMWW micro-filtrate MCR on permeate flux of the AFC40 RO membrane at temperature of 35°C, transmembrane pressure of 30 bar and flow velocity of 4.1 and 6.9 m s⁻¹.

found dependencies of the permeation flux on the independent variables ΔP (transmembrane pressure), T (temperature), u (flow velocity) and MCR. The experimental data points (66 in total) were used in order to predict the six parameters $C_1, C_2, C_3, C_4, C_5, C_6$ of the modelling equation (Eq. (2)):

$$\text{Flux (kg m}^{-2} \text{ h}^{-1}) = \frac{C_1 \times \Delta P \times (C_2 + C_3 \times T + C_4 \times T^2) \times u^{C_5}}{\text{MCR}^{C_6}} \quad (2)$$

The non-linear regression analysis software NLREG (by Phillip H. Sherrod, Member Association of Shareware Professionals (ASP)) was used to predict the values of the parameters. The predicted values are presented in Table 1.

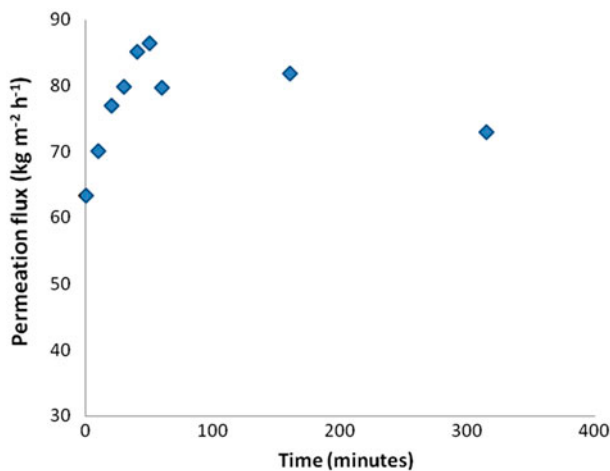


Fig. 8. Permeate flux of the AFC40 RO membrane fluctuation with time (temperature of 35°C, transmembrane pressure of 20 bar and flow velocity of 5.6 m s⁻¹).

Table 1
Predicted values of model parameters

Parameter	Value
C ₁	0.00320650819
C ₂	386.391362
C ₃	19.1462136
C ₄	-0.279068751
C ₅	0.287780952
C ₆	3.76121941

The goodness of the fitness is presented in Fig. 9, where the experimentally measured flux values are plotted against the predicted ones by the model. The correlation between the two parameters is linear and the slope is unity, with $R^2 = 0.97$, thus implying a high-accuracy fitting of the experimental data by the proposed formula.

The model of Eq. (2) is not directly including the osmotic pressure of the concentrated OMWW liquid as the majority of the proposed models for RO applications. However, the introduction of MCR in this model equation, which is a parameter correlated with the osmotic pressure of the OMWW liquid, creates an equivalent effect and takes into account the dependence of the osmotic pressure on the OMWW concentration. This novel modelling approach is more convenient as it does not demand measurements of OMWW osmotic pressure at various concentrations, but instead much simpler flux measurements at various MCRs. This novel approach can also be of general use in RO applications.

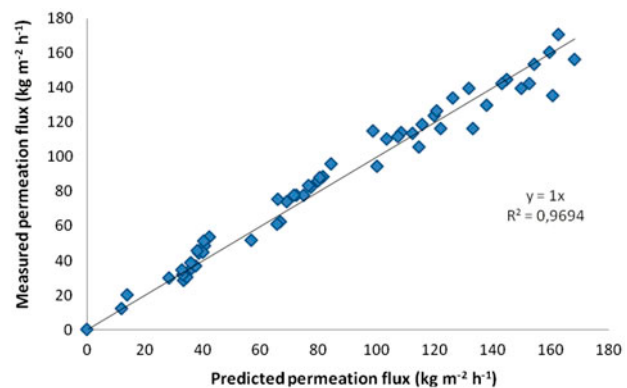


Fig. 9. Correlation of measured and predicted permeate flux of the AFC40 RO membrane, for various conditions of temperature, transmembrane pressure, flow velocity and MCR.

4. Conclusions

In the present work, the use of a dual RO membrane technology scheme in concentrating OMWW was studied at pilot size. In the first step, the tubular (open geometry) commercial RO membrane AFC40 was used to concentrate the OMWW micro-filtrate, which was obtained by OMWW pre-treatment using MF. OMWW micro-filtrate concentration with the AFC40 RO membrane resulted in high flux values without substantial fouling effects. In the second step, the permeate of AFC40 was effectively concentrated using the tubular high rejection commercially available RO membrane AFC99. At the end, clean water was produced as permeate, while the retentate was mixed with the AFC40 retentate to produce a concentrate solution containing the valuable olive fruit antioxidants for commercial utilization in food and cosmetic use.

Regarding the operating conditions of the AFC40 RO membrane, the optimum permeation flux value was 170 kg m⁻² h⁻¹, achieved at transmembrane pressure of 40 bar, temperature of 25°C and flow velocity of 8.3 m s⁻¹. The comprehensive parametric study proved the dependency of permeation flux on transmembrane pressure, operating temperature, flow velocity and MCR. Furthermore, based on the experimental data, a novel mathematical model was successfully developed which can be used for design purposes, and also in various RO applications. According to the proposed model, permeation flux increases linearly with increasing transmembrane pressure, increases exponentially with increasing flow velocity, decreases exponentially with increasing MCR and finally, there is a polynomial second-order dependence of permeation flux on temperature.

Acknowledgements

This research has been financed by the European Union (European Social Fund—ESF) and Greek national funds through the Operational Program “Education and Lifelong Learning” of the National Strategic Reference Framework (NSRF)—Research Funding Program: “ARCHIMEDES III. Investing in knowledge society through the European Social Fund”.

References

- [1] M. Avraamides, D. Fatta, Resource consumption and emissions from olive oil production: A life cycle inventory case study in Cyprus, *J. Cleaner Prod.* 16 (2008) 809–821.
- [2] A. Pavlidou, E. Anastasopoulou, M. Dassenakis, I. Hatzianestis, V. Paraskevopoulou, N. Simboura, E. Rousselaki, P. Drakopoulou, Effects of olive oil wastes on river basins and an oligotrophic coastal marine ecosystem: A case study in Greece, *Sci. Total Environ.* 497–498 (2014) 38–49.
- [3] S. Sklavos, G. Gatidou, A. Stasinakis, D. Haralambopoulos, Use of solar distillation for olive mill wastewater drying and recovery of polyphenolic compounds, *J. Environ. Manage.* 162 (2015) 46–52.
- [4] M. Niaounakis, C.P. Halvadakis, *Olive Processing Waste Management Literature Review and Patent Survey*, second ed., Elsevier, Amsterdam, (2006).
- [5] N. Kalogerakis, M. Politi, S. Foteinis, E. Chatzisyseon, D. Mantzavinos, Recovery of antioxidants from olive mill wastewaters: A viable solution that promotes their overall sustainable management, *J. Environ. Manage.* 128 (2013) 749–758.
- [6] H. Obied, M. Allen, D. Bedgood, P. Prenzler, K. Robards, R. Stockmann, Bioactivity and analysis of biophenols recovered from olive mill waste, *J. Agric. Food Chem.* 53(4) (2005) 823–837.
- [7] M. Tsimidou, G. Papadopoulos, D. Boskou, Phenolic compounds and stability of virgin olive oil—Part I, *Food Chem.* 45(2) (1992) 141–144.
- [8] J.M. Ochando-Pulido, G. Hodaifa, M.D. Victor-Ortega, S. Rodriguez-Vives, A. Martinez-Ferez, Effective treatment of olive mill effluents from two-phase and three-phase extraction processes by batch membranes in series operation upon threshold conditions, *J. Hazard. Mater.* 263 (2013) 168–176.
- [9] S.E. Garrido Hoyos, L. Martínez Nieto, F. Camacho Rubio, A. Ramos Cormenzana, Kinetics of aerobic treatment of olive mill wastewater (OMW) with *Aspergillus terreus*, *Process Biochem.* 37(10) (2002) 1169–1176.
- [10] I.P. Marques, Anaerobic digestion treatment of olive mill wastewater for effluent re-use in irrigation, *Desalination* 137 (2001) 233–239.
- [11] M.S. Fountoulakis, S.N. Dokianakis, M.E. Kornaros, G.G. Aggelis, G. Lyberatos, Removal of phenolics in olive mill wastewaters using the white-rot fungus *Pleurotus ostreatus*, *Water Res.* 36 (2002) 4735–4744.
- [12] B.Y. Ammary, Treatment of olive mill wastewater using an anaerobic sequencing batch reactor, *Desalination* 177 (2005) 157–165.
- [13] M. Taccari, M. Ciani, Use of *Pichia fermentans* and *Candida* sp. strains for the biological treatment of stored olive mill wastewater, *Biotechnol. Lett.* 33 (2011) 2385–2390.
- [14] P. Paraskeva, E. Diamadopoulos, Technologies for olive mill wastewater (OMW) treatment: A review, *J. Chem. Technol. Biotechnol.* 81 (2006) 475–485.
- [15] M. Annesini, F. Gironi, Olive oil mill effluent: Ageing effects on evaporation behaviour, *Water Res.* 25 (1991) 1157–1160.
- [16] E.S. Aktas, S. Imre, L. Ersoy, Characterization and lime treatment of olive mill wastewater, *Water Res.* 35 (2001) 2336–2340.
- [17] K. Al-Malah, M.O.J. Azzam, N.I. Abu-Lail, Olive mills effluent (OME) wastewater post-treatment using activated clay, *Sep. Purif. Technol.* 20 (2000) 225–234.
- [18] J. Cegarra, C. Paredes, A. Roig, M.P. Bernal, D. García, Use of olive mill wastewater compost for crop production, *Int. Biodeterior. Biodegrad.* 38(3–4) (1996) 193–203.
- [19] E.K. Papadimitriou, I. Chatjipavlidis, C. Balis, Application of composting to olive mill wastewater treatment, *Environ. Technol.* 18(1) (1997) 10–107.
- [20] D.L. Bouranis, A.G. Vlyssides, J.B. Drossopoulos, G. Karvouni, Some characteristics of a new organic soil conditioner from the co-composting of olive oil processing wastewater and solid residue, *Commun. Soil Sci. Plant Anal.* 26 (1995) 2461–2472.
- [21] R. Sarika, N. Kalogerakis, D. Mantzavinos, Treatment of olive mill effluents, *Environ. Int.* 31 (2005) 297–304.
- [22] L. Martínez Nieto, G. Hodaifa, S. Rodríguez, J.A. Giménez J. Ochando, Flocculation–sedimentation combined with chemical oxidation process, *Clean—Soil Air Water* 39(10) (2011) 949–955.
- [23] M. Stoller, On the effect of flocculation as pretreatment process and particle size distribution for membrane fouling reduction, *Desalination* 240 (2009) 209–217.
- [24] H. Inan, A. Dimoglo, H. Şimşek, M. Karpuzcu, Olive oil mill wastewater treatment by means of electro-coagulation, *Sep. Purif. Technol.* 36(1) (2004) 23–31.
- [25] Ü. Tezcan Ün, S. Uğur, A.S. Koparal, Ü. Bakır Ögütveren, Electro-coagulation of olive mill wastewaters, *Sep. Purif. Technol.* 52(1) (2006) 136–141.
- [26] J.B. De Heredia, J. Garcia, Process integration: Continuous anaerobic digestion—Ozonation treatment of olive mill wastewater, *Ind. Eng. Chem. Res.* 44 (2005) 8750–8755.
- [27] L. Martínez Nieto, G. Hodaifa, S. Rodríguez, J.A. Giménez, J. Ochando, Degradation of organic matter in olive oil mill wastewater through homogeneous Fenton-like reaction, *Chem. Eng. J.* 173(2) (2011) 503–510.
- [28] G. Hodaifa, J.M. Ochando-Pulido, S. Rodriguez-Vives, A. Martinez-Ferez, Optimization of continuous reactor at pilot scale for olive-oil mill wastewater treatment by Fenton-like process, *Chem. Eng. J.* 220 (2013) 117–124.
- [29] M. Stoller, M. Bravi, Critical flux analyses on differently pretreated olive vegetation waste water streams: Some case studies, *Desalination* 250 (2010) 578–582.
- [30] N. Papastefanakis, D. Mantzavinos, A. Katsaounis, DSA. Electrochemical treatment of olive mill wastewater on Ti/RuO₂ anode, *J. Appl. Electrochem.* 40(4) (2010) 729–737.

- [31] Ü. Tezcan Ün, U. Altay, A.S. Koparal, U.B. Ogutveren, Complete treatment of olive mill wastewaters by electro-oxidation, *Chem. Eng. J.* 139 (2008) 445–452.
- [32] P. Cañizares, L. Martínez, R. Paz, C. Sáez, J. Lobato, M.A. Rodrigo, Treatment of Fenton-refractory olive oil mill wastes by electrochemical oxidation with boron-doped diamond anodes, *J. Chem. Technol. Biotechnol.* 81(8) (2006) 1331–1337.
- [33] P. Grafias, N.P. Xekoukoulotakis, D. Mantzavinos, E. Diamadopoulos, Pilot treatment of olive pomace leachate by vertical-flow constructed wetland and electrochemical oxidation: An efficient hybrid process, *Water Res.* 44(9) (2010) 2773–2780.
- [34] W.K. Lafi, B. Shannak, M. Al-Shannag, Z. Al-Anber, M. Al-Hasan, Treatment of olive mill wastewater by combined advanced oxidation and biodegradation, *Sep. Purif. Technol.* 70(2) (2009) 141–146.
- [35] S. Khoufi, F. Aloui, S. Sayadi, Treatment of olive oil mill wastewater by combined process electro-Fenton reaction and anaerobic digestion, *Water Res.* 40 (2006) 2007–2016.
- [36] L. Rizzo, G. Lofrano, M. Grassi, V. Belgiorno, Pre-treatment of olive mill wastewater by chitosan coagulation and advanced oxidation processes, *Sep. Purif. Technol.* 63(3) (2008) 648–653.
- [37] D.P. Zagklis, A.I. Vavouraki, M.E. Kornaros, C.A. Paraskeva, Purification of olive mill wastewater phenols through membrane filtration and resin adsorption/desorption, *J. Hazard. Mater.* 285 (2015) 69–76.
- [38] C. Russo, A new membrane process for the selective fractionation and total recovery of polyphenols, water and organic substances from vegetation waters (VW), *J. Membr. Sci.* 288 (2007) 239–246.
- [39] E. Garcia-Castello, A. Cassano, A. Criscuoli, C. Conidi, E. Drioli, Recovery and concentration of polyphenols from olive mill wastewaters by integrated membrane system, *Water Res.* 44 (2010) 3883–3892.
- [40] C. Conidi, R. Mazzei, A. Cassano, L. Giorno, Integrated membrane system for the production of phytotherapies from olive mill wastewaters, *J. Membr. Sci.* 454 (2014) 322–329.
- [41] A. El-Abbassi, A. Hafidi, M.C. García-Payo, M. Khayet, Concentration of olive mill wastewater by membrane distillation for polyphenols recovery, *Desalination* 245 (2009) 670–674.
- [42] A. Cassano, C. Conidi, E. Drioli, Comparison of the performance of UF membranes in olive mill wastewaters treatment, *Water Res.* 45 (2011) 3197–3204.
- [43] C. Cassano, L. Conidi, Fractionation of olive mill wastewaters by membrane separation techniques, *J. Hazard. Mater.* 248–249 (2013) 185–193.
- [44] C.A. Paraskeva, V.G. Papadakis, D.G. Kanellopoulou, P.G. Koutsoukos, K.C. Angelopoulos, Membrane filtration of olive mill wastewater and exploitation of its fractions, *Water Environ. Res.* 79 (2007) 421–429.
- [45] C.A. Paraskeva, V.G. Papadakis, E. Tsarouchi, D.G. Kanellopoulou, P.G. Koutsoukos, Membrane processing for olive mill wastewater fractionation, *Desalination* 213 (2007) 218–229.
- [46] H.I. Abdel-Shafy, G. Schories, M.S. Mohamed-Mansour, V. Bordei, Integrated membranes for the recovery and concentration of antioxidant from olive mill wastewater, *Desalin. Water Treat.* 56(2) (2015) 305–314.
- [47] A. Zirehpour, A. Rahimpour, M. Jahanshahi, The filtration performance and efficiency of olive mill wastewater treatment by integrated membrane process, *Desalin. Water Treat.* 53(5) (2015) 1254–1262.
- [48] W. Brand-Williams, M.E. Cuvelier, C. Berset, Use of a free radical method to evaluate antioxidant activity, *LWT-Food, Sci. Technol.* 28(1) (1995) 25–30.